

## A Simple Monte Carlo Method for Locating the Three-dimensional Critical Slip Surface of a Slope

XIE Mowen<sup>1,2</sup>

1 *Institute of Environmental Systems, Kyushu University, Hakozaki 6-10-1, Higashi Ku, Fukuoka, Japan; E-mail: xie@ies.kyushu-u.ac.jp*

2 *College of Resource Engineering, the University of Science and Technology Beijing, 30 Xueyuan Road, Haidian District, Beijing 100083, China*

**Abstract** Based on the assumption of the plain-strain problem, various optimization or random search methods have been developed for locating the critical slip surfaces in slope-stability analysis, but none of such methods is applicable to the 3D case. In this paper, a simple Monte Carlo random simulation method is proposed to identify the 3D critical slip surface. Assuming the initial slip to be the lower part of a slip ellipsoid, the 3D critical slip surface is located by means of a minimized 3D safety factor. A column-based 3D slope stability analysis model is used to calculate this factor. In this study, some practical cases of known minimum safety factors and critical slip surfaces in 2D analysis are extended to 3D slope problems to locate the critical slip surfaces. Compared with the 2D result, the resulting 3D critical slip surface has no apparent difference in terms of only cross section, but the associated 3D safety factor is definitely higher.

**Key words:** three-dimensional slope stability, Monte Carlo simulation, critical slip surface

### 1 Introduction

With the advent of computers, optimization techniques and the Monte Carlo-based random search method have become feasible tools for identifying the critical sliding surface in the slope stability analysis (Baker, 1980; Arai and Tagyo, 1985; Nguyen, 1985; Li and White, 1987; Chen and Shao, 1988). A dynamic programming was proposed by Baker (1980) for locating the critical slip surface by using Spencer's method for calculating the safety factor of a slope. A combined approach (Chen, 1992) uses the random search and the method of optimization to find an estimate of the global minimum.

Greco (1996) used Monte Carlo-based techniques of the random walk type to locate the critical slip surface. Such Monte Carlo-based techniques can be regarded as a direct search approach, which requires calculation of only safety factors and derivatives are not necessary. A new search procedure in generating kinematically admissible slip surfaces was introduced by Malkawi et al. (2001), in which the critical global slip surface as well as its associated safety factor can be determined, and several practical cases have demonstrated the efficiency and capability of the method. Combining the simplified Janbu (1973) method with the principle of optimality, Zhu (2001) proposed an efficient tool for locating the critical slip surface.

All these methods are only used for 2D slope stability analysis, in which an idealized plane-strain section is

selected for analyzing the safety factor of a slope and for locating the 2D critical slip surface. However, any slope failure has a three-dimensional geometry, so it is more rational to treat the slope three-dimensionally for locating the critical slip surface.

Increasing attention has been directed towards the issue and the application of 3D models for assessing slope stability and several 3D analyses have been proposed in geomechanical literature (Hovland, 1977; Chen and Chameau, 1983; Hungr, 1987,1994; Gens et al., 1988; Leshchinsky and Huang, 1992; Lam and Fredlund, 1993; Chen et al., 2001). Most of the 3D methods use a column-based method, in which the differential method is employed to analyze the integration equation of the 3D safety factor by evenly dividing the study area into square columns. Deduced from Hovland's (1977) model, a column-based 3D model will be used for calculating the safety factor in this study. In this model, pore water pressure is considered, and all input data can be easily given in a grid-based form by using the GIS (geography information system) spatial analytical function (Xie et al., 2003).

A simple 3D search method based on the Monte Carlo simulation method is presented here, which assumes the initial slip surface to be the lower part of a slip ellipsoid. The 3D critical slip surface in 3D slope stability analysis is identified by means of a minimization of the 3D safety factor calculated by using the 3D column-based slope-

stability analysis. Some practical cases of known minimum safety factors and critical slip surfaces based on 2D optimization or random techniques are extended to 3D problems in this study to locate the 3D critical slip surface and a comparison was done between the results in these cases with those in 2D cases.

## 2 Random Variables for Monte Carlo Simulation

For detecting the 3D critical slip surface, a search is performed by means of a minimization of the 3D safety factor using the Monte Carlo random simulation method. The initial slip surface is assumed to be the lower part of an ellipsoid slip, and then each randomly produced slip surface is changed according to the strength of different strata and conditions of weak discontinuities. Finally, the critical slip surface will be obtained and, consequently, a relative minimization of the 3D safety factor can be achieved.

The object for locating the critical slip surface is fulfilled by trial searching and calculation of the 3D safety factor. Five parameters related to the size and posture of an ellipsoid are selected as random variables for the Monte Carlo simulation: three axial parameters  $a$ ,  $b$  and  $c$ , central point  $C$  and inclination angle  $\theta$  of the ellipsoid (Fig. 1). If a random produced slip surface is lower than a weak discontinuous surface or the confines of a hard stratum, the weak discontinuity or the confine surface of the hard stratum will be selected as one part of the assumed slip surface. Figure 1 shows that an assumed slip surface is composed of part of the ellipsoid and part of the weak discontinuity.

### 2.1 Three axial parameters of ellipsoid

The geometrical parameters  $a$ ,  $b$  and  $c$  of an ellipsoid are randomly selected in a certain range as in Equation (1):

$$\begin{aligned} a &\in (a_{\min}, a_{\max}) \\ b &\in (b_{\min}, b_{\max}) \\ c &\in (c_{\min}, c_{\max}) \end{aligned} \quad (1)$$

where  $a$ ,  $b$  and  $c$  are assumed to have uniform distribution. From Fig. 1 it is clear that the length of a landslide is equal to  $2a$ , so  $a_{\max}$  is set to be half of the search limit  $L$ .  $2b$  is the width of the landslide. If the ratio of  $b/a$  can be set, the range of  $b$  can also be limited. By analyzing the characteristics regarding the scale of the past 40 landslides in Japan (Fig. 2 shows the distribution of  $b/a$ ), it can be seen that the average value of  $b/a$  is about 0.8. Therefore, the ratio of  $b/a$  is set to be the mode (0.8) of the distribution (Fig. 2) in the following case studies. The value of  $c$  is a

possible depth of the landslide and its range limit can be set by referring to geotechnical information. For randomly selecting all possible slip surfaces, ranges of  $a$  and  $b$  are set based on Equation (2) (considering the possible range of sliding mass and assuming the minimum search limit to be  $L/1.5$ ).

$$\begin{aligned} a_{\max} &= L/2, \quad a_{\min} = a_{\max}/1.5 \\ b_{\max} &= 0.8a_{\max}, \quad b_{\min} = b_{\max}/1.5 \end{aligned} \quad (2)$$

The above range is only taken as a guide for setting the size range of the ellipsoid. No doubt the range can also be set according to the characteristics of a certain slope.

### 2.2 Central point of ellipsoid

Central point  $C$  of the ellipsoid is firstly set at the centroid of the search limit or a researcher-selected point, and then in each trial searching, random walk will change the central point. A random walk direction is one of the eight directions shown in Fig. 3 and is calculated with Equation (3):

$$dir = (8Rnd(i)+1)Mod8 \quad (3)$$

where  $dir=1, 2, \dots, 8$  is one of the eight random walk directions,  $i$  is an integer. The walk step is set to be a length of one grid (a square cell of a column) in the following case studies.

### 2.3 Inclination angle of ellipsoid

The inclination of the ellipsoid agrees with the direction of the slope and the inclination angle  $\theta$  of the ellipsoid is equal to the slope angle. If a slope has complicated topographic characteristics, the inclination of the ellipsoid is set to be the average inclination of the slope as shown in Fig. 4. Since the inclination of the ellipsoid cannot be steeper than that of the slope, the maximum value of  $\theta$  is equal to the average slope angle  $AvrSlope$ , and its minimum value is set to be  $0.5 AvrSlope$  for more possible slip surfaces.

### 2.4 Production of Monte Carlo random variables

The above five parameters are selected as the random variables for Monte Carlo simulation, and the random variables are assumed to have uniform distribution. Each random variable with uniform distribution is calculated by using a random variable in a range of  $[0, 1]$  and is obtained with the method of multiplicative congruity:

$$\begin{aligned} y_i &= ay_{i-1}Mod(m) \\ r_i &= y_i / m \end{aligned} \quad (4)$$

where  $a$  = a constant (positive integer),  $m$  = module,  $r_i$  = random variable with uniform distribution in a range of  $[0, 1]$ . By setting an initial value of  $y_0$ , each random variable  $r_i$  can be obtained. The random variable in a range of  $[a, b]$  is then calculated based on Equation (5),

$$x_i = r_i(b-a) + a \quad (5)$$

where  $x_i$  = random variable in a range of  $[a, b]$ .

### 3 Computational Strategy

For critical slip surface searching, random variables are firstly produced with the Monte Carlo simulation, and each slip surface is calculated on the basis of GIS grid-based data. Then the 3D safety factor for each random trial can be calculated with a GIS grid-based 3D model. Figure 5 is the flow chart for locating the 3D critical slip surface and calculating the associated 3D safety factor. Based on the

range of the five random variables, each random sample is produced by the Monte Carlo random variable producer, and the central point of the ellipsoid is determined by random walk. Through these random samples for detecting the slip surface and calculating the 3D safety factor, the 3D critical slip surface and the associated safety factor can be obtained based on the minimum safety factor obtained with  $n$  times of calculation.

For critical slip identification, a test to find a suitable number of times for the Monte Carlo random calculation was performed, in which the frequency of trial calculation was up to 1000. The change of the minimum 3D safety

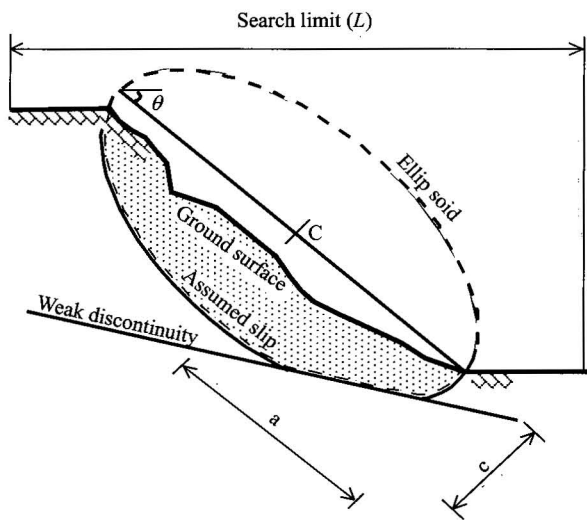


Fig. 1. Ellipsoid for slip surface.

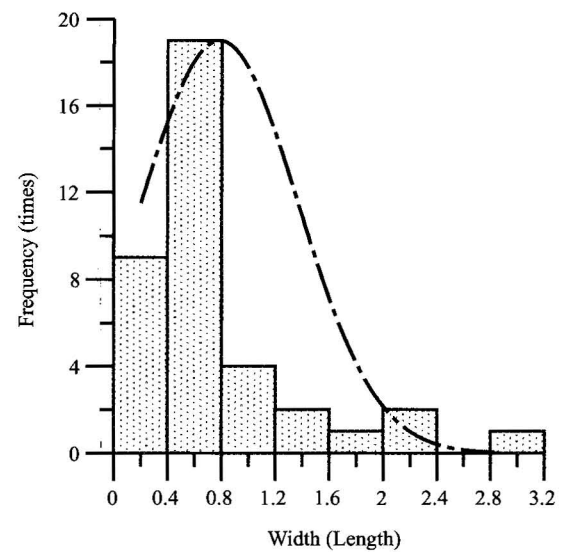


Fig. 2. Distribution of width/length of the 40 past landslides.

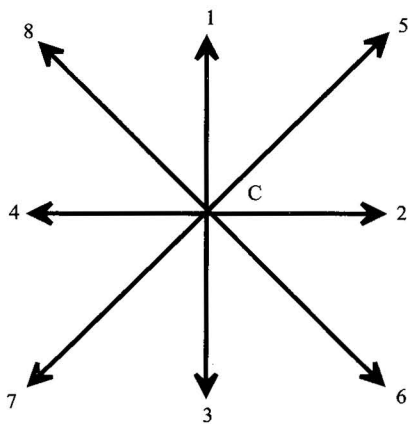


Fig. 3. Eight directions of random walk.

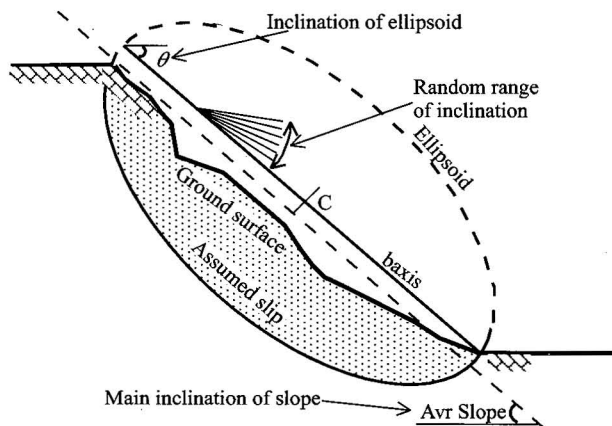


Fig. 4. Inclinations of ellipsoid and slope.

factor of each trial calculation shows that the minimum safety factor can be generally obtained after about 100 trial calculations are performed. In the following case studies the number of times for the calculation is set to be 100.

### 3.1 Coordinate conversion of the ellipsoid

The initial slip surface is assumed to be the lower part of a slip ellipsoid, and the inclination of the ellipsoid is in agreement with the average direction of inclinations over the whole study area. The inclination angle of the ellipsoid is basically set as the main inclination angle (slope angle) of the study area with certain fluctuations. The main direction of inclination  $\alpha$  and the main inclination angle  $\theta$  are determined by the main values of all pixels in the slope failure area (for a simple slope,  $\alpha$  is the inclination direction and  $\theta$  is the slope angle). Let

$$s_1 = \sin \alpha, c_1 = \cos \alpha, s_2 = \sin \theta, c_2 = \cos \theta \quad (6)$$

then the coordinate conversion can be done with equations (7) and (8). Figure 6 shows the process of the coordinate conversion.

**Table 1 Minimum safety factor of case 1**

Method	Range of safety factor
(a) Yamagami and Ueta (1988)	
BFGS	1.338
DFP	1.338
Powell	1.338
Simplex	1.338-1.438
(b) Greco (1996)	
Pattern search	1.327-1.33
Monte Carlo	1.327-1.333
(c) Husein Malkawi et al. (2001)	
Monte Carlo (Random walk)	1.238
(d) This study (3D)	
Monte Carlo (3D)	1.42

**Table 2 Minimum safety factor of case 2**

Method	Range of safety factor
(a) Sridevi and Deep (1991)	
RST-2	0.401
(b) Greco (1996)	
Pattern search	0.388
Monte Carlo	0.388
(c) Husein Malkawi et al. (2001)	
Monte Carlo (Random walk)	0.401
(d) This study (3D)	
Monte Carlo (3D)	0.463

$$\begin{Bmatrix} x \\ y \\ z \end{Bmatrix} = B_3 \cdot B_2 \cdot B_1 \begin{Bmatrix} x \\ y \\ z \end{Bmatrix} + \begin{Bmatrix} -x_0 \\ -y_0 \\ -z_0 \end{Bmatrix} = \begin{bmatrix} c_1 c_2 & -s_1 c_2 & -s_2 \\ s_1 & c_1 & 0 \\ c_1 s_2 & -s_1 s_2 & c_2 \end{bmatrix} \begin{Bmatrix} x-x_0 \\ y-y_0 \\ z-z_0 \end{Bmatrix} \quad (7)$$

$$\begin{Bmatrix} x \\ y \\ z \end{Bmatrix} = \begin{bmatrix} c_1 c_2 & s_1 & c_1 s_2 \\ -s_1 c_2 & c_1 & -s_1 s_2 \\ -s_2 & 0 & c_2 \end{bmatrix} \begin{Bmatrix} x'' \\ y'' \\ z'' \end{Bmatrix} + \begin{Bmatrix} x_0 \\ y_0 \\ z_0 \end{Bmatrix} \quad (8)$$

where  $x, y, z$  refer to the world coordinates;  $x'', y'', z''$ , local coordinates;  $x_0, y_0, z_0$ , the central point of the ellipsoid.

### 3.2 Determination of Z value and inclination angle of the slip surface

The Z value (elevation) of point "B" of the slip surface is determined in terms of the solution of the equation of line AB and the ellipsoid as below (see Fig. 7).

$$\frac{x-x_0}{\sin(\theta)} = \frac{z-z_0}{\cos(\theta)} \quad (9)$$

$$y = y_0$$

$$\frac{x^2}{a^2} + \frac{y^2}{b^2} + \frac{z^2}{c^2} = 1$$

For each pixel, the direction of inclination and the angle of the slip surface are calculated with the following equations, and the inclination of pixel ( $j, i$ ) is calculated based on the Z values of points 1 to 4 in Fig. 8 (Zhou et al., 2001; Xu et al., 2002a; Xu et al., 2002b).

The elevation values of points 1 to 4 are calculated with equations (10) to (12), and the direction of inclination and angle of slip surface are calculated by means of equation (13).

$$\begin{aligned} Z_1 &= [Z(j, i) + Z(j+1, i) + Z(j-1, i-1) + Z(j, i-1)] / 4 \\ Z_2 &= [Z(j, i) + Z(j, i+1) + Z(j+1, i+1) + Z(j+1, i)] / 4 \\ Z_3 &= [Z(j, i) + Z(j, i-1) + Z(j-1, i-1) + Z(j-1, i)] / 4 \\ Z_4 &= [Z(j, i) + Z(j-1, i) + Z(j-1, i+1) + Z(j, i+1)] / 4 \end{aligned} \quad (10)$$

$$\left. \begin{aligned} Z_1 &= (3Z_1 + Z_2 + Z_3 - Z_4) / 4 \\ Z_2 &= (Z_1 + 3Z_2 - Z_3 + Z_4) / 4 \\ Z_3 &= (Z_1 - Z_2 + 3Z_3 + Z_4) / 4 \\ Z_4 &= (-Z_1 + Z_2 + Z_3 + 3Z_4) / 4 \end{aligned} \right\} \quad (11)$$

$$\left. \begin{aligned} a_z &= Z_2 - Z_1 \\ b_z &= Z_3 - Z_1 \end{aligned} \right\} \quad (12)$$

$$\left. \begin{aligned} \tan \theta &= \frac{\sqrt{a_z^2 + b_z^2}}{d} \\ \tan \alpha_0 &= \frac{-a_z}{b_z} \end{aligned} \right\} \quad (13)$$

where  $Z(j, i)$  is the  $Z$  value of pixel  $(j, i)$ ;  $\theta$ , the inclination angle;  $\alpha_0$ , the direction of inclination. When the highest point is point 4, the direction of inclination is  $90+\alpha_0$ ; when the highest point is point 3, the direction of inclination is  $90-\alpha_0$ ; when the highest is point 2, the direction of inclination is  $270-\alpha_0$ ; and when the highest is point 1, the direction of inclination is  $270+\alpha_0$ .

## 4 Case Studies

### Case 1

Case 1 is a homogeneous slope (Fig. 9), which has been studied by numerous researchers. For example, Yamagami and Ueta (1988) used nonlinear programming methods to search for the critical slip surfaces, Greco (1996) employed the Monte Carlo and pattern search methods to locate the critical slip surface, and Malkawi et al. (2001) used the Monte Carlo method of the random walk type for identifying the critical slip surface.

In this study, the case is extended to a simple 3D problem with the same profile and the same geomechanical parameters as those used in the above 2D cases. The study area of  $25 \text{ m} \times 40 \text{ m}$  is divided into 4000 square grid cells (the cell size is  $0.5 \text{ m}$ ) for the GIS spatial analysis. All data relating to the 3D slope stability analysis are based on the grid column. Figure 9 shows the critical slip surface and its 3D safety factor on a 2D profile and in a 3D view. Table 1 summarizes the 3D results obtained here in comparison with 2D results by different researchers. The minimum 3D safety factor is based on 100 times of the Monte Carlo simulation, and the distribution of the 3D safety factor is shown in Fig. 10. The minimum value is 1.42, and the mean and the mode of 100 safety factors are 1.74 and 1.75

respectively. It is clear that the 3D safety factor is higher than those of the 2D results.

The ratio of  $b/a$ , or the ratio of the width to the length of the search limit, is set to be 0.8 for the Monte Carlo simulation in the case studies, and the size of the ellipsoid is randomly changed in the range of the search limit. In this

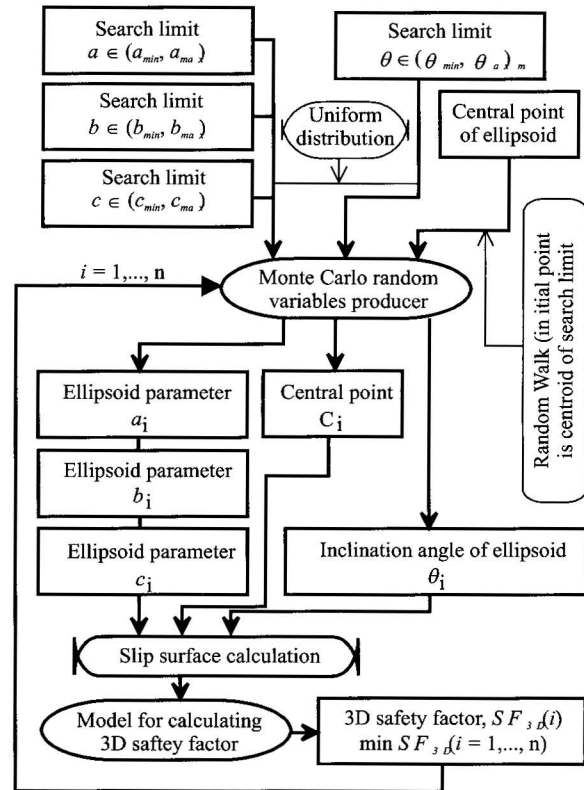


Fig. 5. Flow chart for locating critical slip surface.

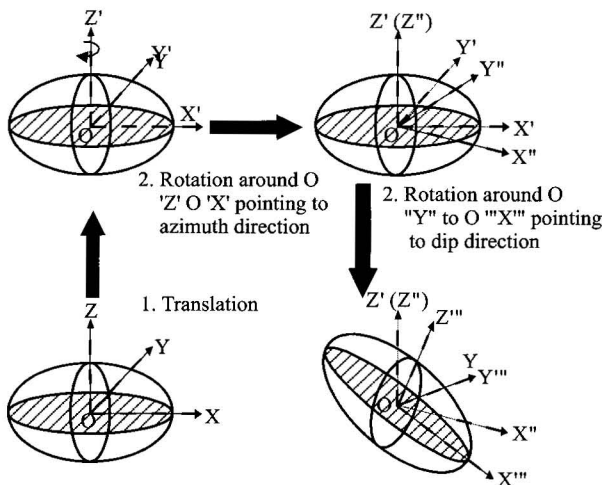


Fig. 6. Coordinate conversion process.

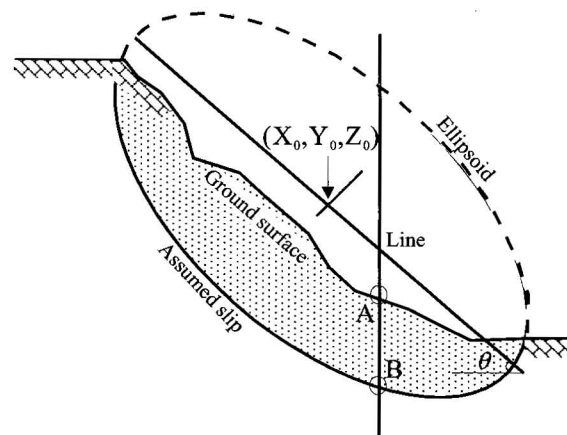


Fig. 7. Calculation of the  $Z$  value of slip surface.

case study, for explaining the relationship of  $b/a$  and the critical 3D safety factor, different  $b/a$  ratios are selected for locating the critical slip and calculating the 3D safety factor. Figure 11 shows the change of the minimum 3D safety factor with increasing  $b/a$ . It can be seen that the 3D safety factor increases sharply with the decrease of  $b/a$  when the ratio of  $b/a$  is smaller than 0.8, and that the 3D safety factor decrease slowly with the increase of  $b/a$  and finally approaches a 2D safety factor when the ratio of  $b/a$  is larger than 0.8. This implies that along with the increase of  $b/a$ , the problem of 3D safety factor calculation is approaching a 2D problem.

## Case 2

In this case, a weak layer is sandwiched between two

strong strata (Fig. 12). The geotechnical properties of layers 1 to 3 are angles of friction  $12^\circ$ ,  $5^\circ$  and  $40^\circ$ , cohesions 29.4, 9.8 and 294.0 kPa, respectively. The unit weight is  $18.82 \text{ kN/m}^3$  for all three layers. This case has been studied by Arai and Tagyo (1985) using Janbu's simplified method in combination with the conjugate gradient method, Sridevi and Deep (1991) using the random search technique RST-2 to locate the critical slip surface, and Greco (1996) and Malkawi et al. (2001) who did identification of the critical slip surface.

This case is extended here to a 3D slope with the same geotechnical properties as used in the above 2D cases. The area for the 3D slope analysis is  $90 \text{ m} \times 96 \text{ m}$ , which is managed by the GIS grid data with a cell size of 0.5 m. Three grid data layers represent the ground surface and the

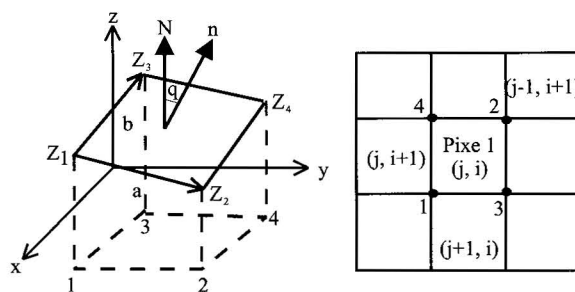


Fig. 8. Calculation of inclination of slip surface.

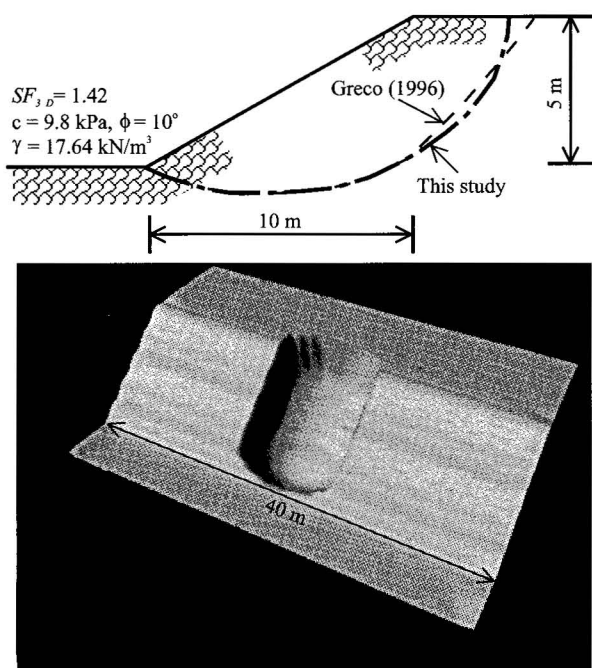


Fig. 9. Critical slip surface of case 1.

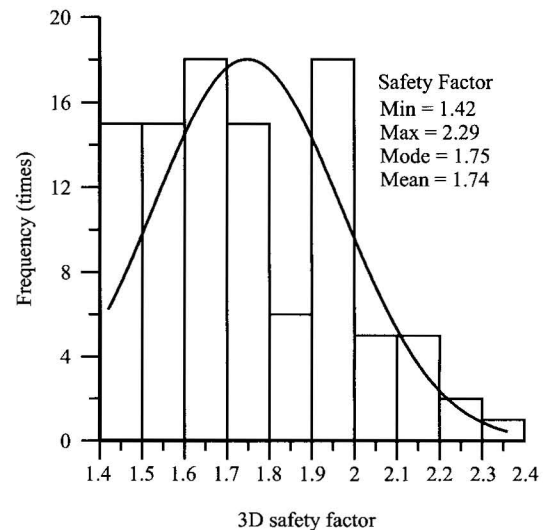


Fig. 10. Distribution of safety factor of 100 times of calculation in case 1.

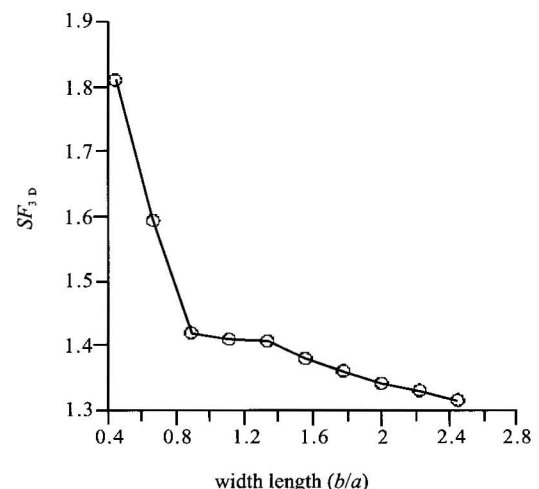


Fig. 11. Minimum safety factor and ratio of width/length.



interfaces of strata, and are handled by a grid-based 3D slope model. Figure 12 shows the critical slip surface in a 2D profile and Fig. 13 shows a 3D view of the critical slip surface. Based on 100 times of the Monte Carlo simulation, the minimum 3D safety factor was obtained, which is 0.463. The distribution of all these 3D safety factors is illustrated in Fig. 14, and the mode and the mean are also shown in this figure. Table 2 summarizes the 2D results obtained by different researchers and the 3D result of this study. The value of the 3D safety factor is about 15% higher than those of the 2D results.

### Case 3

The profile of case 3 is shown in Fig. 15 and the case is related to a slope with an underlain hard stratum whose surface is a weak discontinuity. The geotechnical properties of layers 1 to 4 are respectively: angles of friction  $35^\circ$ ,  $25^\circ$ ,  $30^\circ$  and  $16^\circ$ ; cohesions 9.8, 58.8, 19.8 and 9.8 kPa; and unit weights 19.6, 18.62, 21.07 and 21.07 kN/m<sup>3</sup>. This case was

first analyzed by Chen and Shao (1988) using nonlinear programming methods such as DFP, simplex, and steepest descent. The case was also studied by Greco (1996) using the Monte Carlo method, Malkawi et al. (2001) using the Monte Carlo method of the random walk type, and Zhu (2001) employing the CSF method.

This 2D case is also extended to a 3D slope here, which is analyzed by using a GIS grid-based 3D model and the Monte Carlo simulation for locating the 3D critical slip surface. The area for the 3D slope analysis is extended to 240 m in length and 192 m in width. The 3D slope is digitally represented by five GIS grid layers with a cell size of 2 m. The five grid data layers represent the ground surface, three interfaces of strata and the underground water level. Figure 15 shows the critical slip surface on a profile and the associated 3D safety factor, and the 3D view of the critical slip surface is shown in Fig. 16. The 2D results obtained by different researchers and the 3D result of this study are listed in Table 3. It is apparent that the

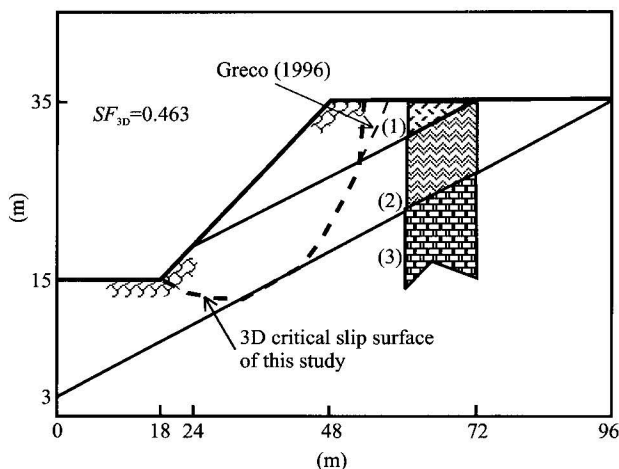


Fig. 12. Critical slip surface and profile of case 2.

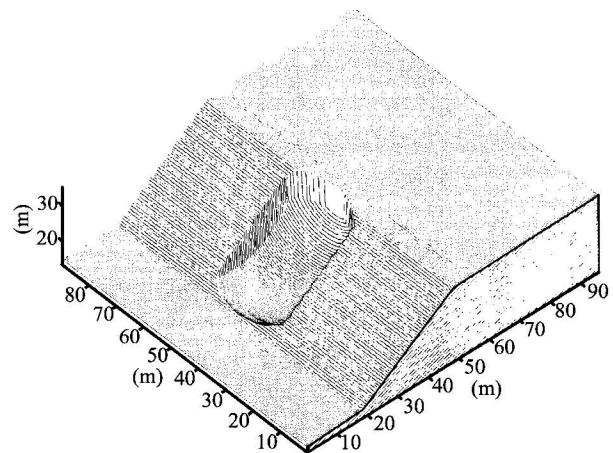


Fig. 13. 3D critical slip surface of case 2.

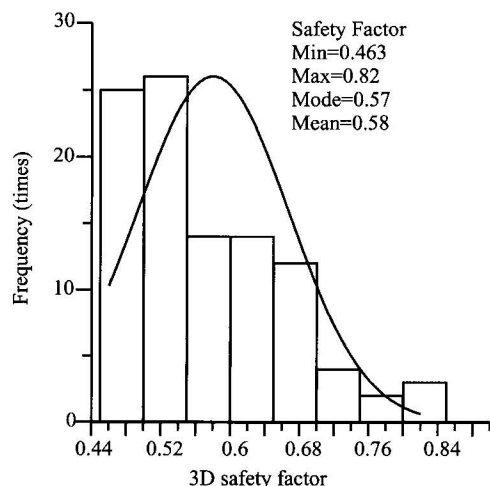


Fig. 14. Distribution of safety factor of 100 times of calculation in case 2.

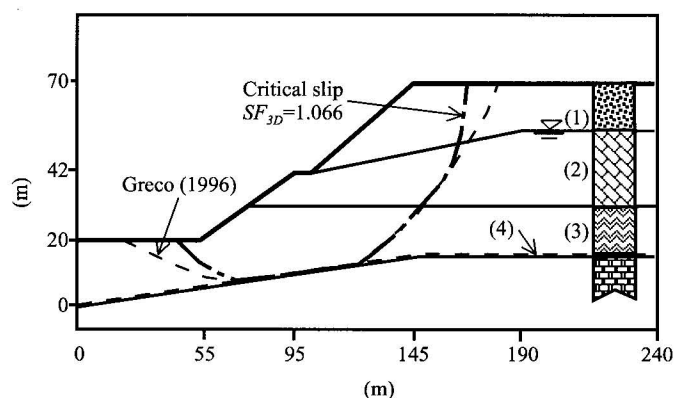


Fig. 15. Critical slip surface and profile of case 3.

value of the 3D safety factor is higher than those of the 2D cases.

#### Case 4

This case involves an earth dam resting on layered soils (Fig. 17). The geotechnical properties of layers 1 to 4 are respectively: angles of friction  $29^\circ$ ,  $30^\circ$ ,  $20^\circ$  and  $30^\circ$ ; cohesions 49, 0, 7.84 and 0 kPa; and unit weights 20.38, 17.64, 20.38 and 17.64 kN/m<sup>3</sup>. As a 2D problem, this case has been studied by many researchers for locating the critical slip surface. Yamagami and Ueta (1988) solved this case by using limiting equilibrium and different minimization procedures. Similarly, Greco (1996) solved it by using Spencer's method and pattern-search and the Monte Carlo technique. Malkawi et al. (2001) analyzed it by using the Monte Carlo method of the random walk type. Zhu (2001) also analyzed this case based on the CSF method.

In order to compare this case with the 2D results, it is also extended to a 3D problem. The Y-direction range is 208 m (X and Z direction ranges are shown in Fig. 17), and the cell size for GIS grid layers is 2 m. The resultant critical slip surface is shown in Fig. 17 in a 2D view and in Fig. 18 in a 3D view. The results of those 2D methods and this 3D method are listed in Table 4. As expected, the 3D result is larger than the 2D results.

#### 5 Conclusions

A new GIS-based 3D searching method based on the Monte Carlo simulation, assuming the initial slip to be the lower part of an ellipsoid, is proposed to locate the 3D critical slip surface in the 3D slope stability analysis. All of the data relating to the calculation of the 3D slope safety factor are in the form of GIS data, therefore it is not necessary to perform data conversion between the GIS form and other forms, and the complex algorithms and iteration procedures of a 3D problem can be perfectly implemented.

Some practical cases of known minimum safety factors and associated critical slip surfaces based on the 2D optimization or random technique are extended to 3D slope problems to identify 3D critical slip surfaces and the result is compared with the 2D results.

In view of only the section of the critical slip surface, no apparent difference can be detected between the results in 3D cases and those in 2D cases, but it is clear that the 3D safety factors are definitely higher than those in 2D cases. The ratio of  $b/a$ , or the ratio of the width to the length of the search limit, has been studied for explaining the relationship of  $b/a$  and the 3D safety factor. This relationship indicates that the suitable limit of  $b/a$  is 0.8,

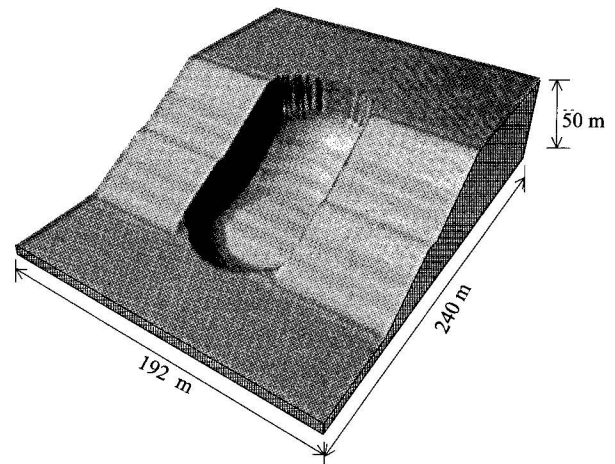


Fig. 16. 3D Critical slip surface of case 3.

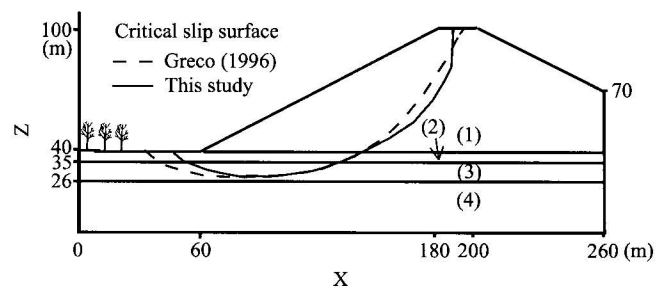


Fig. 17. Critical slip surface and profile of case 4.

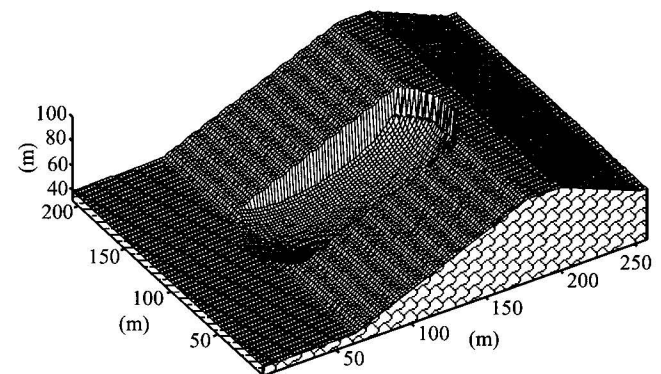


Fig. 18. 3D Critical slip surface of case 4.

and the 3D safety factors will decrease slowly with the increase of  $b/a$ , and finally the 3D safety factor approaches the 2D safety factor.

This paper presents a new approach to locating the critical slip surface in the 3D slope stability analysis, in which all slope-related data are in the form of GIS grid layer. Until now there has not been a well-accepted 3D model for the slope stability analysis, so the comparison of results in different 3D models should be the future work for improving the searching approach. For a slope with complicated strata and discontinuities, the suitable limit of



$b/a$  is not always 0.8. In this case, the proposed approach does not ensure that the result found is the global minimum. It is just a relative one. The probability of detecting a global minimum will increase by setting the limit of  $b/a$  according to the geological and stratigraphic conditions of the study area.

Manuscript received Jan. 21, 2003

accepted Dec 22, 2003

edited by Liu Xinzh

## Reference

- Arai, K., and Tagyo, K., 1985. Determination of non-circular slip surface giving the minimum factor of safety in slope stability analysis. *Soils and Foundations*, 25(1): 43–51.
- Baker, R., 1980. Determination of the critical slip surface in slope stability computations. *Intern. J. Numerical and Analytical Methods in Geomechanics*, 4: 333–359.
- Baligh, M.M., and Azzouz, A.S., 1975. End effects on the stability of cohesive slopes. *J. Geotech. Engineering Division, ASCE*, 101(GT11): 1105–1117.
- Chen, Z.-Y., and Shao, C.-M., 1988. Evaluation of minimum factor of safety in slope stability analysis. *Canadian Geotech. J.*, 25: 735–748.
- Chen, Z.-Y., 1992. Random trials used in determining global minimum factors of safety of slopes. *Canadian Geotech. J.*, 29: 225–233.
- Chen, R., and Chameau, J. L., 1983. Three-dimensional limit equilibrium analysis of slopes. *Geotechnique*, 33: 31–40.
- Chen, Z.Y., Wang, X.G., Heberfield, C., Yin, J.H., and Wang, Y. J., 2001. A three-dimensional slope stability analysis method using the upper bound theorem. *Intern. J. Rock Mechanics & Mining Sciences*, 38: 369–397.
- Gens, A., Hutchison, J.N., and Cavounidis, S., 1988. Three dimensional analysis of slices in cohesive soils. *Geotechnique*, 38: 1–23.
- Greco, V.R., 1996. Efficient Monte Carlo technique for locating critical slip surface. *J. Geotech. Engineering, ASCE*, 122(7): 517–525.
- Hovland, H.J., 1977. Three-dimensional slope stability analysis method. *J. Geotech. Engineering, Division Proceedings of the American Society of Civil Engineers*, 103(GT9): 971–986.
- Hungr, O., 1987. An extension of Bishop's simplified method of slope stability analysis to three dimensions. *Geotechnique*, 37 (1): 113–117.
- Hungr, O., 1994. A general limit equilibrium model for three-dimensional slope stability analysis: discussion. *Canadian Geotech. J.*, 31: 791–795.
- Hungr, O., Salgado, F.M., and Byrne, P.M., 1989. Evaluation of a three-dimensional method of slope stability analysis. *Canadian Geotech. J.*, 26: 679–686.
- Janbu, N., 1973. Slope stability computers. In: Hirschfeld, R.C., and Poulos, S.J. (eds.), *The Embankment Dam Engineering*. New York: John Wiley & Sons, 47–86.
- Lam, L., and Fredlund, D.G., 1993. A general limit equilibrium model for three-dimensional slope stability analysis. *Canadian Geotech. J.*, 30: 905–919.
- Leshchisky, D., and Huang, C.C., 1992. Generalized three dimensional slope stability analysis. *J. Geotech. Engineering*, 118(11): 1748–1763.
- Li, K.S., and White, W., 1987. Rapid evaluation of the critical slip surface in slope stability problems. *Intern. J. Numerical and Analytical Methods in Geomechanics*, 11: 449–473.
- Malkawi, H., A.I., Waleed, F.H., and Sarada, K.S., 2001. Global search method for locating general slip surface using Monte Carlo techniques. *J. Geotech. Geoenviron. Engineering, ASCE*, 8: 688–698.
- Nguyen, V.U., 1985. Determination of critical slope failure surfaces. *J. Geotech. Engineering, ASCE*, 111(2): 238–250.
- Sridevi, B., and Deep, K., 1991. Application of global optimization technique to slope stability analysis. *Proceedings of 6th International Symposium on Landslides*, 573–578.
- Xie, M., Esaki, T., Zhou, G., and Mitani, Y., 2003. Three-dimensional stability evaluation of landslide and a sliding process simulation using a new geographic information systems component. *Environ. Geol.*, 43(5): 503–512.
- Xu Zhiqin, Li Haibing, Chen Wen, Wu Cailai, Yang Jingsui, Jin Xiaochi and Chen Fangyuan, 2002. A large ductile sinistral strike-slip shear zone and its movement timing in the south Qilian Mountains, Western China. *Acta Geologica Sinica* (English edition), 76 (2): 183–193.
- Xu Jiandong, Lin Chiente and Jacobi, R.D., 2002. Characterizing fracture spatial patterns by using semivariograms. *Acta Geologica Sinica* (English edition), 76 (1): 89–99.
- Yamagami, T., and Ueta, Y., 1988. Search for noncircular slip surfaces by the Morgenstern-Price method. *Proceedings of 6th International Conference on Numerical Methods in Geomechanics*, 1219–1223.
- Zhou Yong, Xu Ronghua, Yan Yuehua, Pan Yusheng, Tsanyao Frank Yang, Wei Lo and Wu Chunming, 2001. Dating of the Karakorum strike-slip fault. *Acta Geologica Sinica* (English edition), 75 (1): 10–18.
- Zhu, D.Y., 2001. A method for locating critical slip surfaces in slope stability analysis. *Canadian Geotech. J.*, 38: 328–337.